Optics Letters

High speed OFDM-CDMA optical access network

X. Guo,[1,*] Q. Wang,[1,3] L. Zhou,[2] L. Fang,[2] A. Wonfor,[1] R. V. Penty,[1] and I. H. White[1]

[1]Centre for Photonic Systems, Electrical Engineering Division, Department of Engineering, University of Cambridge, 9 J. J. Thomson Avenue, Cambridge CB3 0FA, UK
[2]Huawei Technologies, Bantian, Longgang District, Shenzhen 518129, China
[3]Department of Electronic Engineering, Tsinghua University, Beijing 100084, China
*Corresponding author: xg218@cam.ac.uk

Received 13 January 2016; revised 9 March 2016; accepted 11 March 2016; posted 14 March 2016 (Doc. ID 257228); published 12 April 2016

We demonstrate the feasibility of a 16 × 3.75 Gb/s (60 Gb/s aggregate) Orthogonal frequency division multiplexing-code division multiple access passive optical network for next-generation access applications. 3.75 Gb/s PON channel transmission over 25 km single-mode fiber shows 0.1 dB dispersion and 0.9 dB crosstalk penalties. Advantages of the system include high capacity, enhanced spectral efficiency, coding gain, and networking functions such as increased security and single-wavelength operation.

OCIS codes: (060.4250) Networks; (060.4510) Optical communications; (060.4080) Modulation.

http://dx.doi.org/10.1364/OL.41.001809

The continuing expansion of bandwidth demand for optical access networks is growing exponentially due to the population of bandwidth-hungry services and applications in recent years, such as high-definition television (HDTV) and 3-D video telephony, online gaming, and cloud computing which demand optical transmission systems with higher spectral efficiency and higher channel data rates. Optical broadband access networks have emerged to address these challenges by supporting scalable and flexible bandwidths enabling multiple services. Next Generation Passive Optical Networks (NG-PONs) are forecast to increase the global capacity of broadband access to well beyond 40 Gb/s downlink and 10 Gb/s uplink levels [1] to meet this need.

However, the computational requirements involved in electronic dispersion compensation for PONs using traditional modulation become very complex and power-hungry as the data rate increases. Orthogonal frequency division multiplexing (OFDM) based PONs are now regarded as promising solutions for future broadband access networks owing to their properties like the high transmission capacity and spectral efficiency, large chromatic and polarization mode dispersion tolerance, and flexible and dynamic bandwidth allocation. In practice, OFDM involves a parallel modulation implementation based on the fast Fourier transform (FFT), which enables modulation format variation on each low bandwidth OFDM subcarrier that can adapt to frequency-dependent channel quality. This also makes possible simple single-tap equalization, significantly reducing the required bandwidth, complexity, and cost of the electronics in the Optical Network Unit (ONU) side [2,3]. Various OFDM PON configurations have been investigated recently. Time division multiplexing OFDM PONs (TDM-OFDM PONs), [4] which enable efficient and dynamic bandwidth allocation but have difficulties at higher transmission speeds and burst synchronization. They also suffer from low security and high interference between different ONUs and the upstream traffic needs a different wavelength assignment owing to the problem of beat noise. Wavelength division multiplexing OFDM PONs (WDM-OFDM PONs) [5] however, can support very high data rates thanks to multiple wavelengths, but are relatively expensive and complex owing to the use of arrayed waveguide gratings and multiple high-speed OFDM transceivers. They also do not allow flexible and dynamic resource allocation at different ONUs. Code division multiple access (CDMA) technologies have many attractive features such as single-wavelength operation, high power budget margins, a secure physical layer, low interference between users, and low optical beat noise between different channels [6]. If the OFDM-based transmitters and receivers are encoded and decoded with orthogonal codes, they can benefit from dense subcarrier spacing, ease of equalization, multiple access, and crosstalk cancellation. Hence the combination of OFDM and CDMA has been shown to be a potential important evolution route for future low-cost and high-speed NG-PONs [7,8]. Building on this concept, we implement a system using an OFDM modulation scheme which then encounters CDMA encoding/decoding separately for each user for high-aggregate data rates. In addition, the feasibility of a higher number of users is demonstrated.

Figure 1 shows the proposed OFDM-CDMA PON architecture. For the downlink direction, the optical line terminal (OLT) generates unique encoded OFDM data streams with orthogonal codes for different users, and these are simultaneously transmitted to the ONUs. Each user has a corresponding unique CDMA modem which decodes its own data, while the interference between multiple users can be eliminated through a code auto- and cross-correlation process in decoding. The decoded data is then demodulated by an OFDM modem. A similar process can also be employed in the uplink to enable bidirectional transmission. This architecture provides several benefits, including simple implementation, improved spectral efficiency, and security. In particular, it is possible to use a single

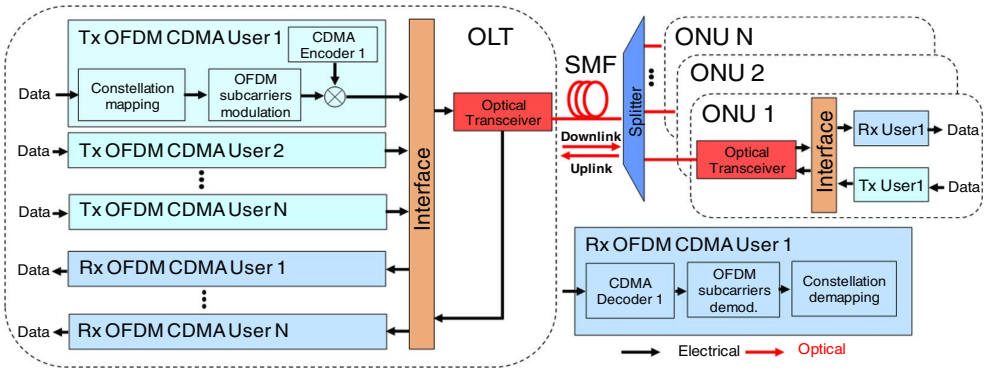

Fig. 1. Proposed architecture of OFDM-CDMA PON.

standard source and detector at the central office to support all users as they share a single wavelength which allows optimization of existing infrastructure and simplifies network management. The correlation properties of the decoding process in a CDMA system also have the potential to improve receiver sensitivity and increase power budgets due to coding gain. This may allow the CDMA signal to be transmitted over longer distances than required in access networks without amplification, thus making possible the integration of access systems with metropolitan area networks (MANs).

Walsh–Hadamard sequences are commonly used for CDMA networks due to their good auto- and cross-correlation properties [6]. For this OFDM-CDMA PON demonstration, a family of Walsh–Hadamard sequences with 16 chips is used. The Walsh–Hadamard codes are defined by the Hadamard matrices of dimension 2^j for $j \in N_a$ (N_a is positive integer) given by the recursive formula below:

$$H(2^j) = \begin{bmatrix} H(2^{j-1}) & H(2^{j-1}) \\ H(2^{j-1}) & -H(2^{j-1}) \end{bmatrix} = H(2) \otimes H(2^{j-1}) \quad (1)$$

for $2 \le j \le N_a$, where $\otimes$ denotes the Kronecker product. The lowest order of Hadamard matrix of two forms the base matrix:

$$H(2^1) = \begin{bmatrix} 1 & 1 \\ 1 & -1 \end{bmatrix}. \quad (2)$$

For the CDMA encoding and decoding process, different codes (rows of the Walsh–Hadamard matrix) are assigned to different users, and a single lth code from the Walsh–Hadamard matrix is expressed as follows:

$$\mathbf{c}^l = [c_0^l \ldots c_{M-1}^l], \qquad l = 1, \ldots, M, \quad (3)$$

where M denotes the length of the code.

Digital OFDM symbols can be expressed as the output of the inverse FFT (IFFT) with the complex number:

$$\mathbf{x} = [x_0 x_1 x_2 \ldots x_{N-1}]^T \quad (4)$$

$$x_n = \frac{1}{\sqrt{N}} \sum_{k=1}^{N} X_k \exp\left(\frac{j2\pi nk}{N}\right), \quad n = 0, 1, \ldots, N-1, \quad (5)$$

where N is the size of the IFFT.

Different from [7,8], the signals are mapped into all the OFDM subcarriers and then the OFDM symbols in each user are spread and encoded using a unique Walsh–Hadamard code rather than the reverse order. Now the nth CDMA encoded OFDM symbol can be written as

$$y_q = c^l_{\mathrm{mod}(q,M)} x_{\lfloor q/M \rfloor}, \qquad q = 0, 1, 2, \ldots MN - 1. \quad (6)$$

Mod () and $\lfloor\rfloor$ denote the modulus after division and floor process in mathematics. Different users can be transmitted simultaneously and, finally, in the decoding process, the corresponding Walsh–Hadamard code is used to distinguish each other via auto- and cross-correlation properties.

In the OFDM-CDMA PON experiments, the PRBS bits are mapped to Quadrature Amplitude Modulation (QAM) symbols and then input onto the OFDM subcarriers via a 512-size IFFT. The subcarriers are arranged so that the 2 subcarriers closest to the optical carrier are omitted. The remaining 510 subcarriers have Hermitian symmetry so that the IFFT output is real-valued for intensity modulation-direct detection (IM-DD), though at the cost of lower spectral efficiency. A cyclic prefix (CP) of 3% is added in front of each OFDM symbol to mitigate the inter-symbol interference (ISI). The complete signal sequence comprises 340 OFDM frames (covering all the subcarriers) in which 40 frames are the training pilots for the estimation of channel subcarriers and phase equalization coefficients. 256 pseudo-noise (PN) bits are inserted in front of the OFDM symbols for automatic system timing synchronization, utilizing their strong cross-correlation properties. Each user is encoded with different 16-bit Walsh–Hadamard codes so that, ideally, 16 users can be transmitted simultaneously. Four typical 16-bit Walsh–Hadamard codes covering different spreading bandwidths are used in this proof-of-principle demonstration.

Code3:{+1+1−1−1+1+1−1−1+1+1−1−1+1+1−1−1}

Code5:{+1+1+1+1−1−1−1−1+1+1+1+1−1−1−1−1}

Code6:{+1−1+1−1−1+1−1+1+1−1+1−1−1+1−1+1}

Code9:{+1+1+1+1+1+1+1+1+1−1−1−1−1−1−1−1−1}

The parameters for these OFDM-CDMA PON experiments are summarized in Table 1.

Simulations are carried out first with the same channel data rate (3.75 Gb/s) and CDMA parameters as used in the experiments in order to validate the feasibility of the proposed OFDM-CDMA PON architecture. In order to perform correlation, the decoder is set with the reverse of the transmitted chip code. For example, if Code 5 is used in the transmitter, the decoder must be configured using Code 5R: {−1 −1 −1 −1 +1 +1 +1 +1 −1 −1 −1 −1 +1 +1 +1 +1}. The transmitted code then causes the filter to output a high-energy signal at the desired sampling point. Figures 2(a1)–2(c1) show the simulation results of the single users encoded with code 5, the

Table 1. OFDM-CDMA PON Experimental Parameters

OFDM-CDMA PON Parameters	
Number of bits	179520
FFT size	512
Subcarrier bandwidth	39 MHz
Single user data rate	3.75 Gb/s/2.5 Gb/s
Modulation	64 QAM/16 QAM
Subcarriers	2–256
OFDM frames	300
Training frames	40
Synchronization	256-bit PN sequence
CP ratio	3%
CDMA	16-bit Walsh–Hadamard codes

combined two-user system (code 3 and code 5), and the combined four-user system (code 3, code 5, code 6, and code 9), respectively, but in the absence of noise for the sake of clarity. Figures 2(a2)–2(c2) show the signal in these three scenarios decoded using code 5R, respectively, with bit-error-rate (BER) measured to be 1×10^{-3}, which is the FEC limit. Figures 2(d1) and 2(d2) show the 64 QAM constellation of decoded signal using code 5R in the four-user system at no error and BER of 1×10^{-3} two scenarios.

Figure 3 shows the OFDM-CDMA PON experimental configuration to validate the proposed architecture. We only demonstrate downstream transmission in this Letter due to equipment limitations. The OFDM-CDMA data is generated offline by Matlab and output by an Arbitrary Waveform Generator (AWG) with a fixed sampling rate of 20 GS/s throughout all the experiments. The data modulates a 1550 nm DFB laser via a 20 GHz $LiNbO_3$ Mach–Zehnder modulator (MZM). The DFB laser is an ILX Lightwave 79800D C-band module with full power of 10 dBm and wavelength/attenuation accuracy of ± 0.05 nm/$\pm$ 0.1 dB. The resulting optical signal is then transmitted through 25 km of single-mode fiber (SMF), EDFA and an optical bandpass (BF) filter, before being detected by a 20 GHz receiver (−15 dBm sensitivity at 10 Gb/s NRZ). The resulting electrical signal is then amplified by a low-noise RF amplifier and sampled by a 100 GS/s real-time scope for DSP offline processing.

The channel frequency response of different OFDM subcarriers is estimated first for the case where the power of all the subcarriers modulated by BPSK is equal. The SNR is estimated at an optical power of −10 dBm and is shown in Fig. 4 as a function of subcarrier number. It can be seen that the subcarriers occupying high frequencies suffer from larger losses, which reflect the whole system frequency response. Adaptive bit and power loading is applied to improve the spectral efficiency.

Figure 5 shows the BER measurements for pure OFDM signals for back-to-back (B2B) operation and after 25 km of SMF. The spectral efficiency is measured to be 1.62 bit/s/Hz and the total data rate is 32.4 Gb/s. There is a negligible 0.1 dB measured power penalty, which indicates good dispersion tolerance. Figure 5 also depicts the BER curves of 64 QAM OFDM-CDMA one- and two-user cases (code 5 and 9) after 25 km of SMF. In order to simplify the experiment, all the subcarriers the adaptive power/bit loading are not applied. It is clearly shown that there is about a 2.8 dB improvement when CDMA coding is applied and this will increase further if a lower order modulation format is used. Despite there being a 3 dB power-splitting loss for two users, there is nearly no measured crosstalk penalty for two simultaneous users. The BER performance is better than the FEC limit in each case. Figure 5 also shows the constellation maps of received 64 QAM signal at BERs of 1.1×10^{-3} and 2×10^{-4}, respectively, for the two-user system. The spectral efficiency is 3 bit/s/Hz and a single-user data rate can achieve 3.75 Gb/s, showing the potential for a record high aggregate data rate of 60 Gb/s.

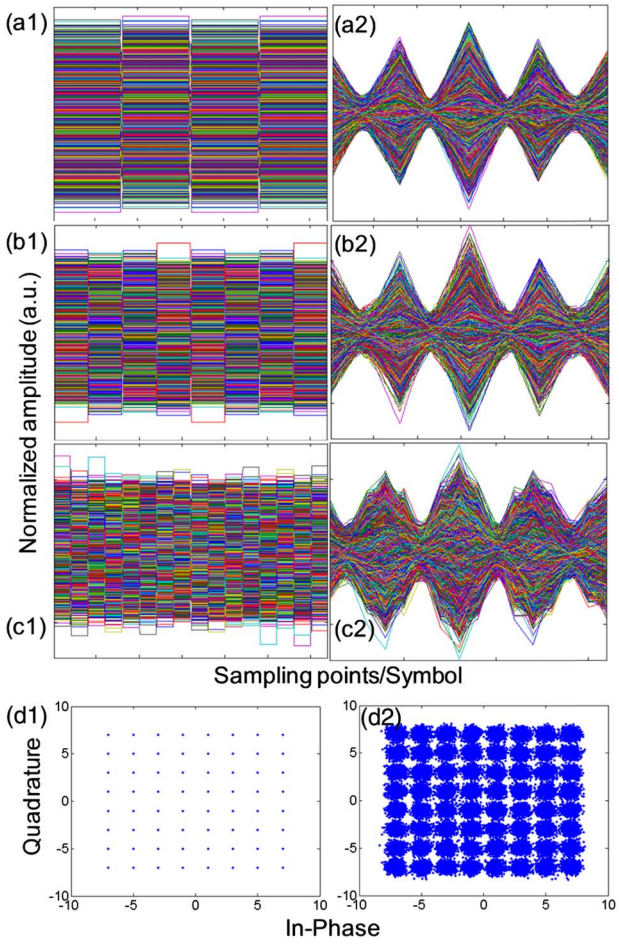

Fig. 2. (a1)–(c1) Simulation of 64 QAM OFDM symbols with single user (encoded with code 5), combined two users (encoded with code 3 and code 5), and combined four users (encoded with code 3, code 5, code 6, and code 9). (a2)–(c2) Simulation of decoded signals using code 5R in single-, two-, and four-user systems, respectively, at BER of 1×10^{-3}. (d1) and (d2) Simulation of 64 QAM constellation of decoded signals using code 5R in four-user system at no error and BER of 1×10^{-3} two scenarios.

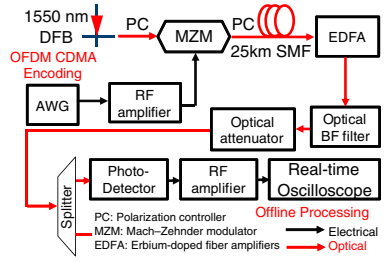

Fig. 3. OFDM-CDMA PON experimental setup (downlink).

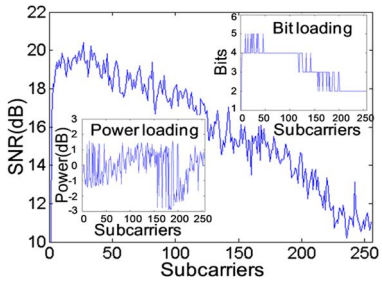

Fig. 4. OFDM SNR measurement as a function of subcarrier number with bit and power loading shown in the insets.

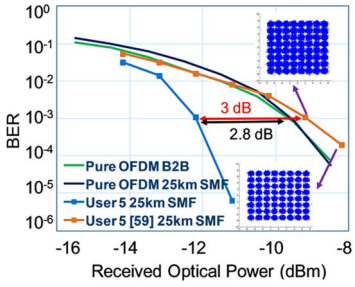

Fig. 5. BER measurements of pure OFDM transmission B2B and after 25 km of SMF, and 64 QAM OFDM CDMA after 25 km with single user 5, and user 5 out of two users (Insets: 64 QAM constellation with BER of 1.1×10^{-3} and 2×10^{-4}).

More users of 64 QAM, however, cannot be demonstrated due to the experimental system noise floor consideration that is worse than the FEC limit. Figure 6 shows the BER curves of 64 QAM OFDM-CDMA user 5 decoded in four-user system (code 3, code 5, code 6, and code 7) after 25 km of SMF and the simulation results under the same noise floor situation. It is found that the BERs measured cannot hit the FEC limit and will become stable at around above 1×10^{-3}. Simulation has been done with a fixed noise floor setting with Signal-to-noise-ratio (SNR) of 18 dB (BER at 1×10^{-3}) then converted to optical power as in experiments. The simulation results fit the experiments well. Hence, in order to support more users, the power penalty has to be decreased, so in the following experiments the modulation format is then changed to 16 QAM.

Figure 7 shows the BER curves for a 16 QAM OFDM-CDMA PON that supports one, two, and four users, with an additional 3 dB splitting loss for each case. However, when comparing user 5 and user 9 in a one-user system, two-user

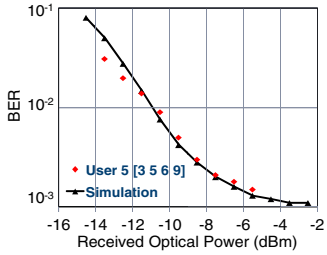

Fig. 6. BER measurements of 64 QAM OFDM CDMA after 25 km with user 5 out of four users and simulation results with fixed noise floor.

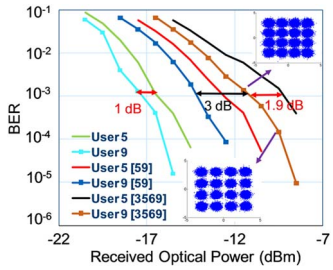

Fig. 7. BER measurements of 16 QAM OFDM CDMA after 25 km with one, two, and four users (Insets: 16 QAM constellations with BER of 1.4×10^{-3} and 1.5×10^{-4}).

system, and four-user system, there are increasing penalties of 1 dB, 1.5 dB, and 1.9 dB at a BER of 1×10^{-3}, respectively. This is because different spreading codes have different frequency bandwidths and hence suffer from different losses as shown in Fig. 4. As a result, they have different SNRs even in the one-user system. Also, as the user number increases, dispersion and crosstalk degrade the channel orthogonality, causing a higher power penalty. The spectral efficiency in this system however, decreases to 2 bit/s/Hz with a single-user data rate of 2.5 Gb/s, but still shows the viability of 16 ONU channels with an aggregate data rate of 40 Gb/s. This could be increased further if more advanced orthogonal codes, higher order modulation formats, or higher code chip rates were used. Of course this also requires a more complex synchronization scheme.

We have proposed and demonstrated the feasibility of a novel OFDM-CDMA PON architecture. Two and four users out of 16-user system have been demonstrated with a maximum single channel data rate of 3.75 Gb/s and a potential aggregate data rate 60 Gb/s. The dispersion penalty is about 0.1 dB and crosstalk penalty is 0.9 dB for four users after 25 km of SMF. The coding gain is 2.8 dB for a 64 QAM OFDM-CDMA single user compared to the case without CDMA, and this can be improved further with a lower order modulation format. This architecture has the benefits of multiple users' access with bidirectional transmission, coding gain for high power budget margins, spectral efficiency, and networking functions with a single wavelength.

Funding. Huawei Technologies.

Acknowledgment. We acknowledge Tektronix for supplying arbitrary waveform generator (AWG70001A).

REFERENCES

1. Y. Luo, X. Zhou, F. Effenberge, X. Yan, G. Peng, Y. Qian, and Y. Ma, J. Lightwave Technol. **31**, 587 (2013).
2. N. Cvijetic, J. Lightwave Technol. **30**, 384 (2012).
3. J. Armstrong, J. Lightwave Technol. **27**, 189 (2009).
4. H. Yang, J. Li, B. Lin, Y. Wan, Y. Guo, L. Zhu, L. Li, Y. He, and Z. Chen, J. Lightwave Technol. **31**, 2735 (2013).
5. X. Hu, L. Zhang, P. Cao, K. Wang, and Y. Su, Opt. Express **20**, 8071 (2012).
6. K. Kitayama, *Optical Code Division Multiple Access: A Practical Perspective* (Cambridge University, 2014).
7. L. Zhang, X. Xin, B. Liu, J. Yu, and Q. Zhang, Opt. Express **18**, 18347 (2010).
8. L. Fang, L. Zhou, X. Liu, X. Zhang, M. Sui, F. Effenberger, and J. Zhou, Opt. Express **23**, 13499 (2015).